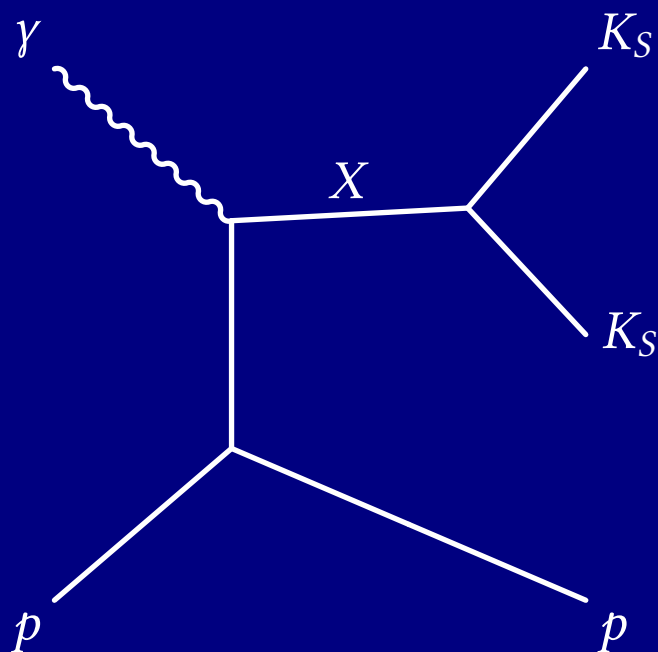

INTRODUCTION TO $K_S K_S$ PHYSICS AT GLUEX



NATHANIEL DENE HOFFMAN

CARNEGIE MELLON UNIVERSITY

Table of Contents

1	Introduction	1
1.1	A Brief History of Particle Physics	2
1.2	Thesis Overview	3
1.3	Motivation	3
1.4	Past Analyses	5
2	Experimental Design and Data Selection	7
2.1	The GlueX Experiment	7
	The GlueX Kinematic Fit	7
2.2	Data Selection for the $K_S K_S$ Channel	7
	Fiducial Cuts	7
2.3	sPlot Weighting	7
3	Partial-Wave Analysis	13
3.1	Amplitude Formalism	14
	Single-Particle Helicity States	14
	Two-Particle Helicity States	16
	Production Amplitudes	17
3.2	Second attempt	17
	Including Linear Polarization	18
3.3	The Z_ℓ^m Amplitude	18
3.4	The K -Matrix Parameterization	18
3.5	Waveset Selection	18
4	Results and Systematic Studies	19
4.1	Mass-Independent Fits	19

4.2	Mass-Dependent Fits	19
4.3	Systematics	19
5	Conclusion	21
A	Derivation of the Chew-Mandelstam Function	23

Chapter 1

Introduction

1.1 A Brief History of Particle Physics

Since the days of the ancient Greeks, scientists and philosophers alike have been interested in the fundamental question concerning the composition of the universe. While the Greeks maintained that the world was composed of four indivisible elemental substances (fire, earth, air, and water) [**aristotle_metaphysics_350bce**], this was at best a guess by the early philosophers, who had no mechanism with which to test their theory. Ironically, these philosophers struggled with a question to which us modern physicists still have no answer: Are the building blocks of the natural world fundamental (indivisible) [**aristotle_physics_350bce**]?

In 1808, John Dalton published a manuscript which described what is now called the "law of multiple proportions" after compiling several observations on chemical reactions which occur with specific proportions of their reactants. He anglicized the Greek *atomos*, meaning "not able to be cut", into the word we are familiar with—"atom" [**dalton_new_1808**]. Towards the end of the century, J. J. Thomson demonstrated that cathode rays could be deflected by an electrostatic field, an observation which could not be explained by the prevailing theory that the rays were some form of light [**thomson_cathode_1897**]. Instead, he proposed that these rays were made up of charged particles he called "corpuscles" (later renamed to the familiar "electrons") [**thomson_corpuscular_1907**]. Around the same time (between 1906 and 1913), Ernest Rutherford, Hans Geiger, and Ernest Marsden conducted experiments in which they scattered alpha particles through a thin metal foil, and, through an analysis of the scattering angles, concluded that a positively charged nucleus must exist at the center of atoms, surrounded by electrons [**rutherford_lxxix_1911**].

Over the next several decades, the nucleus was further divided into protons and neutrons¹ [**masson_xxiv_1921**, **chadwick_possible_1932**]. In 1964, Murray Gell-Mann and George Zweig proposed a theory that protons and neutrons (and all other baryons and mesons) were in fact composed of smaller particles Gell-Mann called "quarks"² [**gell-mann_schematic_1964**]. These particles, along with the electron-like family of leptons (including neutrinos), the gauge bosons, and the Higgs boson, discovered in 2012 [**aad_observation_2012**], comprise the Standard Model, a mathematical model which describes all the known forces and matter of the universe, with the notable exceptions (at time of writing) of gravity, dark matter, dark energy, and neutrino masses.

This thesis begins at a time when physicists are working hard to find gaps in this model, mostly by probing higher and higher ranges of energy. The experimental work being done at GlueX, however, resides in a lower energy regime, which we usually describe as "medium energy physics". As I will elucidate later in this manuscript, the strong force is non-perturbative in this regime, making direct calculations through the Standard Model all but impossible. However, since the advent of Lattice Quantum Chromodynamics (LQCD) in 1974 [**wilson_confinement_1974**],

¹For the discovery of the electron and neutron, Thomson and James Chadwick won Nobel Prizes in Physics in 1906 and 1935, respectively. Rutherford won the 1908 Nobel Prize in Chemistry for his research in radiation. However, I want to emphasize that while I mention the "big names" here, there are many who contributed in relative obscurity.

²Upon reading the section of Finnegans Wake which Gell-Mann cites as inspiration behind the name, I found (somewhat surprisingly) that the word "quark" was originally intended to rhyme with "mark", "ark", "lark", "bark", and so on, viz. [kwɑːrk] rather than the more common [kwɔːrk]!

physicists have been able to make approximate predictions via computer simulations of the theory.

1.2 Thesis Overview

Herein, I will focus on a particular portion of the Standard Model that dictates the strong interaction, viz. interactions between quarks and gluons, the mediating gauge boson of the strong force. Beginning with a discussion of the theory and history of K_S (K-short) pair production in prior experiments, I will give a brief overview of the GlueX experiment. I will then outline some of the theoretical underpinnings and implications of glueballs to persuade the reader on the importance of this production channel in the larger scheme of GlueX.

Next, I will describe my own analysis, beginning with the the impetus of this study, a search for Σ^+ baryons using a different recombination of the final state in this channel. This will lead to a first-order peek at the many resonances which decay to K_S pairs, and I will delineate the layers of data selection which I have carried out to produce a clean sample of events.

I will then discuss the process of partial-wave analysis (PWA), modeling resonances, and selecting a waveset for my data. I will conclude with the results from fits of these models to the data, the implications of such fits, and the next steps which I or another future particle physicist might take in order to illuminate another corner of the light mesonic spectrum.

1.3 Motivation

While this will be discussed in detail later, I believe it is important to emphasize the motivation for such a study of photoproduction of $K_S K_S$. While the majority of GlueX research concerns the study of hybrid mesons (mesons with forbidden quantum numbers), such mesons cannot be found in this channel. Given a bound state of two spin- $\frac{1}{2}$ quarks with relative angular momentum L , total spin S and total angular momentum J (the eigenvalue of $\hat{J}^2 = \hat{L}^2 \oplus \hat{S}^2$), we can define the parity operator \hat{P} by its effect on the wave function of the system,

$$\hat{P} |\vec{r}\rangle = \eta |\vec{r}\rangle \quad (1.1)$$

where η can be determined by noting that states of angular momentum are generally proportional to a spherical harmonic in their angular distribution ($|r, \theta, \varphi; LM\rangle \sim Y_L^M(\theta, \varphi)$) and

$$\hat{P} Y_L^M(\theta, \varphi) = Y_L^M(\pi - \theta, \pi + \varphi) = (-1)^L Y_L^M(\theta, \varphi) \quad (1.2)$$

so $\eta = (-1)^L$. The Dirac equation can be used to show that the intrinsic parity of quarks and antiquarks, when multiplied, yields a factor of -1 , so

$$\hat{P} |q\bar{q}; J L M S\rangle = -(-1)^L \quad (1.3)$$

Similarly, the operator \hat{C} representing C-parity will also introduce a factor of $(-1)^L$ because exchanging charges of a (neutral³) quark-antiquark system is akin to reversing their positions under parity. If $|S\rangle$ is antisymmetric under C-parity, we should get an additional factor of -1 , which is the case for the $S = 0$ singlet. With the aforementioned -1 due to the intrinsic parity of the quarks and antiquarks, we find

$$\hat{C}|q\bar{q};JLMS\rangle = (-1)^{L+S} \quad (1.4)$$

Labeling states with the common J^{PC} notation, it can then be shown that states like 0^{--} , 0^{+-} , 1^{--} , and 2^{+-} (among others) are not allowed states for $q\bar{q}$ mesons. As mentioned, the investigation of such states is the primary focus of the GlueX experiment. However, since the particle we are concerned with decays to two identical particles (K_S) which have a symmetric spatial wave function, and because this particle is a meson which follows Bose-Einstein statistics, the angular part of the total wave function must also be symmetric, i.e. $J = \text{even integers}$. Furthermore, because parity is conserved in strong decays, and the state of two identical particles is symmetric under parity, the decaying meson must also have $P = +$. Finally, the strong interaction also conserves C-parity, and both kaons are neutral, so we can determine the J^{PC} quantum numbers of the resonance to be even⁺⁺. There should be no overlap here with the aforementioned hybrid mesons, but that does not mean the channel is not of interest to GlueX and the larger scientific community. Particularly, the lowest lying glueball states are predicted to not only share these quantum numbers, but exist in the middle of the mass range produced by GlueX energies[[morningstar_glueball_1999](#)]. To add to this, the spin-0 isospin-0 light flavorless mesons, denoted as f_0 -mesons, are supernumerary, either due to mixing with a supposed light scalar glueball or by the presence of a light tetraquark (or both)[[particle_data_group_review_2020](#)].

However, it would be an understatement to say that the $K_S K_S$ channel at GlueX is not the ideal place to be looking for either glueballs or tetraquarks. This is because, while we have excellent handles for reconstructing this channel, we have no ability to separate particles of different isospin with these data alone. This means that these f states will be indistinguishable from their isospin-1 partners, the a -mesons. At first glance, it might seem like a model of the masses of these particles would make it easy to separate them, even if they remained indistinguishable between resonant peaks, but with broad states like the $f_0(1370)$ and states which sit right on top of each other (like the $f_0(980)$ and $a_0(980)$, which also tend to interfere with each other), there is likely no unique mass model which can distinguish all of the possible states without relying on data from other channels.

The silver lining is that, due to the GlueX detector's state-of-the-art angular acceptance[[adhikari_glueX_2021](#)], we do stand a chance at separating spin-0 states from spin-2 states, and GlueX's polarized beam allows us to further understand the mechanisms at play by giving us some indication of the parity of the t -channel exchanged particle in the production interaction. We can also use this channel as a proving ground for more complex amplitude analysis involving a mass model, which could be extended to a coupled-channel analysis in the future.

³For \hat{C} to be Hermitian, and thus observable, acting it twice on a state should return the original state, so only eigenvalues of ± 1 are allowed. Therefore, only states which are overall charge neutral are eigenstates of \hat{C} .

1.4 Past Analyses

This is certainly not the first attempt to disentangle the $K_S K_S$ channel. In 1967, Beusch et al. published their observation of a resonance in the “ $K_1^0 K_1^0$ ” system. An analysis of 1,560 events in a spark chamber. In 1979, ANL published an analysis of the channel $\pi^- p \rightarrow K_S K_S n$ examined 5,096 events with a mass-independent fit to several partial waves. In 1982, the TASSO collaboration at the DESY storage ring PETRA published an analysis of $e^+ e^- \rightarrow e^+ e^- + f'$ where f' decays to charged pions via a pair of K_S^0 s [CITE TASSO]. This channel is typically thought of as production from photon fusion, $\gamma\gamma \rightarrow K_S K_S$. Their analysis, over an integrated luminosity of 79pb^{-1} (roughly 100 events in the final selection of data between 1.2 and 1.9 GeV), was just sensitive enough to see a peak from what they referred to as the $f'(1515)$. They assumed this was a spin-2 resonance, consistent with the modern $f'_2(1525)$. Many of the f and a states had not yet been discovered at this time, though they include an “ f^0 ” and “ A_2 ” in their fit, likely the modern $f_2(1270)$ and $a_2(1320)$ ⁴. In 1982 and 1986, BNL measured the $\pi^- p \rightarrow K_S K_S n$ channel and performed partial-wave analyses with 15,359 and 40,494 events, respectively. The first of these measurements fit a set of Breit-Wigners for the S^* ($f_0(980)$), f ($f_2(1270)$), A_2 ($a_2(1320)$), ϵ ($f_0(1500)$), f' ($f'_2(1525)$), $S^{*'}(f_0(1710))$, and a G-wave particle called h (now the $f_4(2050)$). The second took a different approach, using a K -matrix formalism over just the D-wave resonances using poles corresponding to an $f_2(1270)$ and $f'_2(1525)$ as well as a $\theta(1690)$ and $f_r(1810)$ which do not appear to correspond to any modern known resonances. Two years later, the PLUTO collaboration, also at PETRA, would re-examine the photon-fusion channel, emphasizing the $f_2(1270)$, $a_2(1320)$, $f'_2(1525)$, $f_2(1720)$, and $X(2230)$ states [CITE PLUTO]. Around the same time, the LASS collaboration at SLAC published their analysis via the $K^- p \rightarrow K_S K_S \Lambda$ (hypercharge exchange). Using a sample of 441 events, they appear to be the first to discover evidence for an S-wave near the $f'_2(1525)$, a state we now refer to as the $f_0(1500)$. The next year, the CELLO collaboration (again at PETRA) would publish their analysis on the $\gamma\gamma \rightarrow K_S K_S$ channel consisting of 30 events.

In 1995, the L3 collaboration at LEP would present their analysis of the photon-fusion channel [CITE LEP 1995]. Their data, the culmination of data collected over the years 1991 through 1994, amounted to 62 events after all selections, half of which were determined to be consistent with an $f'_2(1525)$. Five years later, LEP would present a new analysis with 802 events [CITE LEP 2000]. This was the first analysis to see a clear peak from the $f_2(1270)/a_2(1320)$ region, as well as a signal from the $f_f(1710)$ (whose spin was not yet determined). No f_0 states like LASS’s $f_0(1500)$ were included in the analysis, and this is not surprising, LEP’s angular acceptance makes these states indistinguishable from a combination of spin-2 states with helicity-0 and -2. Additionally, $SO(3)$ arguments show that the isospin-0 f -states and the isospin-1 a -states should interfere destructively in $K_S K_S$ decays, so some overlapping states such as

⁴Strangely, the only f -meson known at the time was the $f(1270)$. In Figure 2a from [CITE], it appears that there are two peaks in the fit. The lower peak at around 1.3 GeV is likely the $A_2(1320)$, now called the $a_2(1320)$. The higher peak has the $f'(1515)$ of course, but there is no f^0 around either mass peak listed in the 1982 PDG, and there are still no spin-0 f -mesons listed in the 1984 PDG. [CITE 1982, and 1984 PDG] However, the CELLO paper on production of the $f_0(1270)$ [CITE CELLO 1986] two years later would seem to indicate that the spin of this resonance was not well known at the time. BNL’s 1986 paper also refers to a D-wave f particle with a mass of 1.277 GeV [CITE BNL 1986]

the $f_0(980)/a_0(980)$ were simply not visible in these analyses due to interference. In 2006, LEP would release another analysis of this channel, this time with 870 events, this time mentionaing a signal from the $f_0(980)/a_0(980)$ [CITE Schegelsky LEP 2006].

Chapter 2

Experimental Design and Data Selection

2.1 The GlueX Experiment

The GlueX Kinematic Fit

2.2 Data Selection for the $K_S K_S$ Channel

Fiducial Cuts

2.3 sPlot Weighting

At this stage in the analysis, we are running low on simple cuts which can improve the signal-to-background ratio in the dataset. We must now turn to more complex solutions of separating the signal from potential background seepage. The first method we will use to do this is `sPlot`[`pivk_splot_2005`]¹, a weighting scheme which corrects the naïve probabilistic weights one might first think to construct (dubbed “inPlot”).

We start by developing a model for the signal and background probability distribution functions (PDFs) for a “discriminating” variable. We could then weight each event by some normalized probability of it being in the signal distribution rather than the background:

$$w(x) = \frac{N_S f_S(x)}{N_S f_S(x) + N_B f_B(x)} \quad (2.1)$$

where x is the discriminating variable, $f_S(x)$ and $f_B(x)$ are the corresponding signal and background PDFs, and N_S and N_B are the total number of signal and background events, respectively.

However, as shown by Pivk and Le Diberder[`pivk_splot_2005`], we must be careful when using this procedure, as it will only correctly produce signal-isolated plots for “control” variables y which are directly correlated with x . For the time being, let us assume that this is not the case, and that we wish to use the distribution of some variable which is uncorrelated with the variables we are plotting and analyzing². Following the `sPlot` derivation, we find that, to plot uncorrelated control variables, we must weight our data according to the following scheme:

$$w(x) = \frac{V_{SS} f_S(x) + V_{SB} f_B(x)}{N_S f_S(x) + N_B f_B(x)}, \quad \text{where } V_{ij}^{-1} = \sum_x \frac{f_i(x) f_j(x)}{(N_S f_S(x) + N_B f_B(x))^2} \quad (2.2)$$

The V^{-1} matrix can also be understood as the covariance matrix between the free parameters N_S and N_B in the fit of the signal-background mixture, $V_{ij}^{-1} = -N \frac{\partial^2 \ln \mathcal{L}}{\partial N_i \partial N_j}$, although there is reason to believe this will lead to less accurate results than the manual calculation in ??[`dembinski_custom_2022`].

Now that we have a method of assigning weights, we must pick the discriminating variable. Typically, these weighting methods work well on the classic “bump-on-a-background” distributions, but because the mass of the kaons is constrained in the kinematic fit, the fitted mass of each kaon is just a δ -function and combination of measured masses for each $\pi^+ \pi^-$ pair will yield a Normal distribution with little to no apparent background (by construction). We must be a bit more clever in determining a discriminating variable! By examining the BGGEN analysis done in [TODO: PREVIOUS SECTION], we can see that most likely sources of background arise when the intermediate kaons are missing from the reaction: $\gamma p \rightarrow 4\pi p$. This reaction shares the $K_S K_S$ final state exactly, so pairs of pions which look close enough to kaons will be almost indistinguishable in the data. However, they differ in one key way, namely that the K_S intermediate contains a strange quark while the $\pi^+ \pi^-$ decay state does not, so such a decay must occur via the weak interaction, which is notably slower than the strong interaction which would produce pion

¹This is stylized as *sPlot* in the original paper, but I find this tedious to type and to read.

²We will later see that things are not quite so simple!

pairs with no intermediate kaon. In other words, while the signal's rest-frame lifetime distribution should have an exponential slope near the K_S lifetime, the background would theoretically have nearly zero rest-frame lifetime for every event, or a much smaller exponential slope in practice.

Therefore, we will begin by generating both a signal and background dataset in Monte Carlo. We then interpret both datasets as if they were our desired channel by running them through the GlueX reconstruction and reaction filter, as well as all of our selections up to this point. We can then fit the rest-frame lifetime of each dataset to an exponential model,

$$f(t) = \lambda \exp\{-\lambda t\} \quad (2.3)$$

where $\lambda \equiv 1/\tau$, the lifetime of the kaon in question. Since we have two independently decaying kaons, we should really form a joint distribution for both, where we will assume each kaon has the same average lifetime:


$$f(t_1, t_2) = \lambda^2 \exp\{-\lambda t_1\} \exp\{-\lambda t_2\} \quad (2.4)$$

Both the signal and background distributions can be modeled in this way, giving us only two free parameters, λ_S and λ_B for the signal and background respectively, to fit (see [Figure 2.1](#) for an example of these fits).

Once we obtain nominal values for λ_S and λ_B from fits over the signal and background Monte Carlo, we can fix the exponential slopes to the fit values and perform a new fit to our real data with a mixture model (see [Figure 2.2](#)):

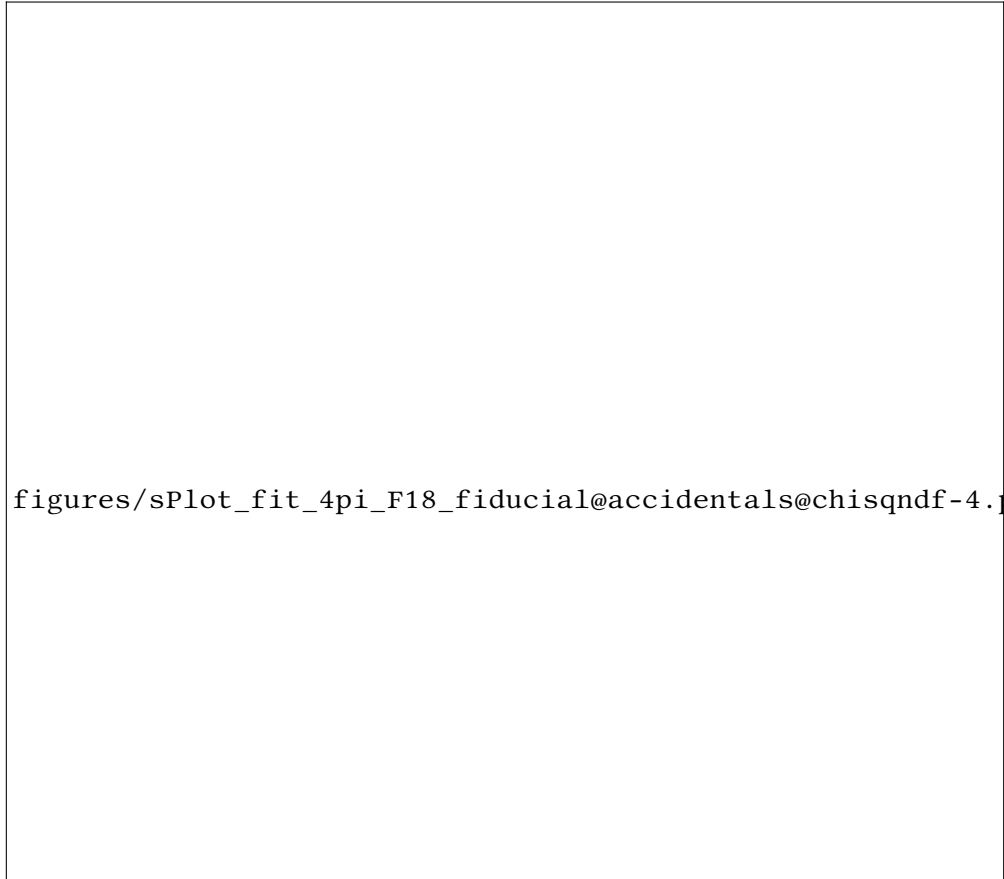
$$f(t_1, t_2) = z \lambda_S^2 \exp\{-\lambda_S t_1\} \exp\{-\lambda_S t_2\} + (1 - z) \lambda_B^2 \exp\{-\lambda_B t_1\} \exp\{-\lambda_B t_2\} \quad (2.5)$$

In the fit to data, only the fraction of signal to background, z , is floating. From its fit value, we can determine values of N_S and N_B to use in [Equation \(2.2\)](#) and complete the weighting procedure.



figures/sPlot_fit_accmc_F18_fiducial@accidentals@chisqndf-4.png

(a)



figures/sPlot_fit_4pi_F18_fiducial@accidentals@chisqndf-4.png

Figure 2.2: Fit of Equation (2.5) to data from the F18 run period. True kaon events are prominent in the tail of the distribution, which does not appear in background Monte Carlo samples (Figure 2.1b) TODO: zoom axis to 0.2

Chapter 3

Partial-Wave Analysis

3.1 Amplitude Formalism

TODO: cite <http://scipp.ucsc.edu/~haber/ph218/ExperimentersGuideToTheHelicityFormalism.pdf> and S.U. Chung spin formalisms

Now we embark on the topic of amplitudes. We wish to describe the dynamics of our reaction in a way that allows us to extract quantum numbers like spin from our data. There are several difficulties in doing so: First, we are trying to determine the properties of many particles at once, and we know that many resonances in this channel overlap in mass space. This precludes the use of a simple Breit-Wigner description of most of these resonances, as overlapping Breit-Wigners do not preserve unitarity TODO: citation. Second, the GlueX experiment uses a linearly polarized photon beam, so it behooves us to use a formalism which can include this polarization. Finally, there are many resonances in this channel, and while we have the largest photoproduction dataset to date, we are still relatively data limited, which further complicates any dynamical description.

Single-Particle Helicity States

We begin by defining a set of observables which are independent of frames and rotations on those frames. This is known as the helicity formalism, where helicity resembles the spin projection along the axis of a particle's motion. First, we define a rotation $R(\alpha, \omega, \gamma)$ as a matrix whose action on a vector is a rotation about the Euler angles α , ω , and γ . For each rotation, we can define a unitary operator $U[R]$ which has the group property $U[R_2 R_1] = U[R_2] U[R_1]$ as it is an operator on the group $SO(3)$. Being an operator on $SO(3)$, we can also write it as

$$U[R(\alpha, \omega, \gamma)] = e^{-i\alpha J_z} e^{-i\omega J_y} e^{-i\gamma J_z} \quad (3.1)$$

We can then describe the matrix elements of this operator in the angular momentum eigenbasis $|jm\rangle$ (representing a spin- j particle where m is the projection of spin onto the \hat{z} -axis) with the Wigner D-matrix:

$$U[R(\alpha, \omega, \gamma)] \equiv \sum_{m'} |jm\rangle D_{m'm}^j(R(\alpha, \omega, \gamma)) \quad (3.2)$$

where

$$D_{m'm}^j(\alpha, \omega, \gamma) \equiv e^{-im'\alpha} d_{m'm}^j e^{-im\gamma} \quad (3.3)$$

and

$$d_{m'm}^j(\omega) = \langle jm' | e^{-i\omega J_y} | jm \rangle \quad (3.4)$$

We can further extend this eigenbasis to include linear momentum by introducing Lorentz boosts $L(\vec{\beta})$. We denote the operation of a boost along the \hat{z} -axis with velocity β as $L_z(\beta)$. A boost in any direction described by

polar angles (θ, φ) can be achieved by rotating the \hat{z} -axis to align with the direction vector, boosting in the new \hat{z} -direction, and rotating back:

$$L(\vec{\beta}) = R(\varphi, \theta, 0)L_z(\beta)R^{-1}(\varphi, \theta, 0) \quad (3.5)$$

Together, the space of rotations and boosts defines the Lorentz group, where each arbitrary Lorentz transformation Λ has a unitary operator $U[\Lambda]$ with the group property $U[\Lambda_2\Lambda_1] = U[\Lambda_2]U[\Lambda_1]$, so in terms of operators, we can also write

$$U[L(\vec{p})] = U[R(\varphi, \theta, 0)]U[L_z(p)]U^{-1}[R(\varphi, \theta, 0)] \quad (3.6)$$

Finally, this allows us to define the “canonical” basis for a single particle as

$$U[L(\vec{p})]|jm\rangle \equiv |\vec{p}, jm\rangle \quad (3.7)$$

Unfortunately, the quantum number m is only valid in the rest frame of the state because the \hat{z} -axis of the rest frame is not equivalent to the \hat{z} -axis in any arbitrarily Lorentz-transformed frame. Therefore, we will define helicity λ as the projection of spin along the direction of motion and introduce new helicity states,

$$|\vec{p}, j\lambda\rangle = U[L(\vec{p})]U[R(\varphi, \theta, 0)]|j\lambda\rangle = U[R(\varphi, \theta, 0)]U[L_z(p)]|j\lambda\rangle \quad (3.8)$$

In this definition, we have two ways of obtaining the helicity frame: We can either rotate the state first such that the quantization axis is aligned with \vec{p} and then boost in the \hat{p} -direction or we can first boost in the \hat{z} -direction and then rotate. In either equivalent case, λ is invariant under rotations as well as boosts parallel to \vec{p} . Finally, we can define these helicity states over a basis of canonical states:

$$|\vec{p}, j\lambda\rangle = \sum_m D_{m\lambda}^j(R(\varphi, \theta, 0))|\vec{p}, jm\rangle \quad (3.9)$$

The single-particle states are normalized such that

$$\begin{aligned} \langle \vec{p}', j'\lambda' | \vec{p}, j\lambda \rangle &= \tilde{\delta}(\vec{p}' - \vec{p})\delta_{j'j}\delta_{\lambda'\lambda} \\ \text{with } \tilde{\delta}(\vec{p}' - \vec{p}) &= (2\pi)^3(2E)\delta^{(3)}(\vec{p}' - \vec{p}) \end{aligned} \quad (3.10)$$

since the Lorentz-invariant phase space element is given by $\tilde{d}p = \frac{d^3p}{(2\pi)^3(2E)}$. This gives the following representation of the identity:

$$\sum_{j\lambda} \int |\vec{p}, j\lambda\rangle \tilde{d}p \langle \vec{p}, j\lambda| = I \quad (3.11)$$

Two-Particle Helicity States

Of course, we would like to extend these states to be able to talk about interactions and decays. For notation, I will use Ω to represent the polar angles θ and φ and \emptyset to describe the specific value of 0 for both of these angles. Similarly, R_Ω and R_\emptyset will represent the corresponding rotation operators (the second being a null rotation the direction of the \hat{z} -axis). R without subscript or angles will represent an arbitrary rotation whose angles are not important for the derivation.

Next, we can define a joint state of two particles with masses w_1 and w_2 (to avoid confusion with angular momenta) and spins s_1 and s_2 . In the center-of-momentum (COM) frame, these particles are back-to-back, and we can define the momentum of particle 1 as \vec{p} with direction Ω and particle 2 as $-\vec{p}$. Then the joint canonical state, up to a normalization constant \mathcal{N} , is given by

$$|\Omega, s_1 m_1 s_2 m_2\rangle = \mathcal{N} U[L(\vec{p})] |s_1 m_1\rangle U[L(-\vec{p})] |s_2 m_2\rangle \quad (3.12)$$

Such a state can also be described with a total spin s and moment m_s :

$$|\Omega, sm_s\rangle = \sum_{m_1 m_2} (s_1 m_1 s_2 m_2 | sm_s) |\Omega, s_1 m_1 s_2 m_2\rangle \quad (3.13)$$

Here, $(s_1 m_1 s_2 m_2 | sm_s)$ is the Clebsch-Gordan coefficient describing the angular momentum coupling. Next, we can add additional angular momentum apart from the spin. For a system with angular momentum ℓ with moment m , we use the fact that $\langle \Omega | \ell m \rangle = Y_\ell^m(\Omega)$ (spherical harmonics) to define

$$|\ell m sm_s\rangle = \int d\Omega Y_\ell^m(\Omega) |\Omega; sm_s\rangle \quad (3.14)$$

Next, the spin s and angular momentum ℓ can be coupled into the total angular momentum J with moment M :

$$|JM \ell m sm_s\rangle = \sum_{m m_s} (\ell m sm_s | JM) |\ell m sm_s\rangle \quad (3.15)$$

This coupled state is still in the canonical formalism, and we would like to use the helicity basis. Using [Equation \(3.8\)](#),

$$|\Omega, s_1 \lambda_1 s_2 \lambda_2\rangle = \mathcal{N} U[R_\Omega] \underbrace{(U[L_z(p)] |s_1 \lambda_1\rangle U[L_{-z}(p)] |s_2, -\lambda_2\rangle)}_{|\emptyset, s_1 \lambda_1 s_2 \lambda_2\rangle} \quad (3.16)$$

To obtain states with a total angular momentum, we can integrate over the space of all rotations, weighted by Wigner D-matrices:

$$|JM s_1 \lambda_1 s_2 \lambda_2\rangle = \frac{N_J}{2\pi} \int dR D_{M\mu}^{J*}(R) U[R] |\emptyset, s_1 \lambda_1 s_2 \lambda_2\rangle \quad (3.17)$$

This is, of course, incomplete, as we have not defined the normalization factor N_J or the coupling μ which relates helicities to total angular momentum. To do both, let us specify the rotation R as follows,

$$\begin{aligned}
|JM s_1 \lambda_1 s_2 \lambda_2\rangle &= \frac{N_J}{2\pi} \int dR D_{M\mu}^{J*}(R) U[R(\varphi, \theta, \gamma)] |\emptyset, s_1 \lambda_1 s_2 \lambda_2\rangle \\
&= \frac{N_J}{2\pi} \int dR D_{M\mu}^{J*}(R) U[R(\varphi, \theta, 0)] U[R(0, 0, \gamma)] |\emptyset, s_1 \lambda_1 s_2 \lambda_2\rangle \\
&= \frac{N_J}{2\pi} \int dR D_{M\mu}^{J*}(R) e^{-i(\lambda_1 - \lambda_2)\gamma} U[R(\varphi, \theta, 0)] |\emptyset, s_1 \lambda_1 s_2 \lambda_2\rangle \\
&= \frac{N_J}{2\pi} \int d\Omega d\gamma e^{iM\varphi} d_{M\mu}^{J*} e^{i\mu\gamma} e^{-i(\lambda_1 - \lambda_2)\gamma} U[R(\varphi, \theta, 0)] |\emptyset, s_1 \lambda_1 s_2 \lambda_2\rangle \\
&= \frac{N_J}{2\pi} \int d\Omega d\gamma e^{iM\varphi} d_{M\mu}^{J*} e^{i(\mu - (\lambda_1 - \lambda_2))\gamma} |\Omega, s_1 \lambda_1 s_2 \lambda_2\rangle \\
&= N_J \int d\Omega D_{M\lambda}^{J*}(R_\Omega) |\Omega, s_1 \lambda_1 s_2 \lambda_2\rangle
\end{aligned} \tag{3.18}$$

with $\lambda = \lambda_1 - \lambda_2$

It can be shown that the normalization $\mathcal{N} = \frac{1}{4\pi} \sqrt{\frac{p}{w}}$ where p is the relative momentum and w the effective mass of the two-particle system. The normalization of the standard two-particle states is given by

$$\langle \Omega', s'_1 \lambda'_1 s'_2 \lambda'_2 | \Omega, s_1 \lambda_1 s_2 \lambda_2 \rangle = \delta^{(2)}(\Omega' - \Omega) \delta_{s'_1 s_1} \delta_{\lambda'_1 \lambda_1} \delta_{s'_2 s_2} \delta_{\lambda'_2 \lambda_2} \tag{3.19}$$

This follows immediately from [Section 3.1](#). Next, to ensure that

$$\langle J' M' s'_1 \lambda'_1 s'_2 \lambda'_2 | JM s_1 \lambda_1 s_2 \lambda_2 \rangle = \delta_{J' J} \delta_{M' M} \delta_{s'_1 s_1} \delta_{\lambda'_1 \lambda_1} \delta_{s'_2 s_2} \delta_{\lambda'_2 \lambda_2} \tag{3.20}$$

we must have $N_J = \sqrt{\frac{2J+1}{4\pi}}$. Finally,

$$\langle \Omega, s'_1 \lambda'_1 s'_2 \lambda'_2 | JM s_1 \lambda_1 s_2 \lambda_2 \rangle = N_J D_{M\lambda}^{J*}(R_\Omega) \delta_{s'_1 s_1} \delta_{\lambda'_1 \lambda_1} \delta_{s'_2 s_2} \delta_{\lambda'_2 \lambda_2} \tag{3.21}$$

Production Amplitudes

TODO: cite <https://link.springer.com/article/10.1140/epjc/s10052-020-7930-x>

3.2 Second attempt

Following <https://onlinelibrary.wiley.com/doi/10.1155/2020/6674595>

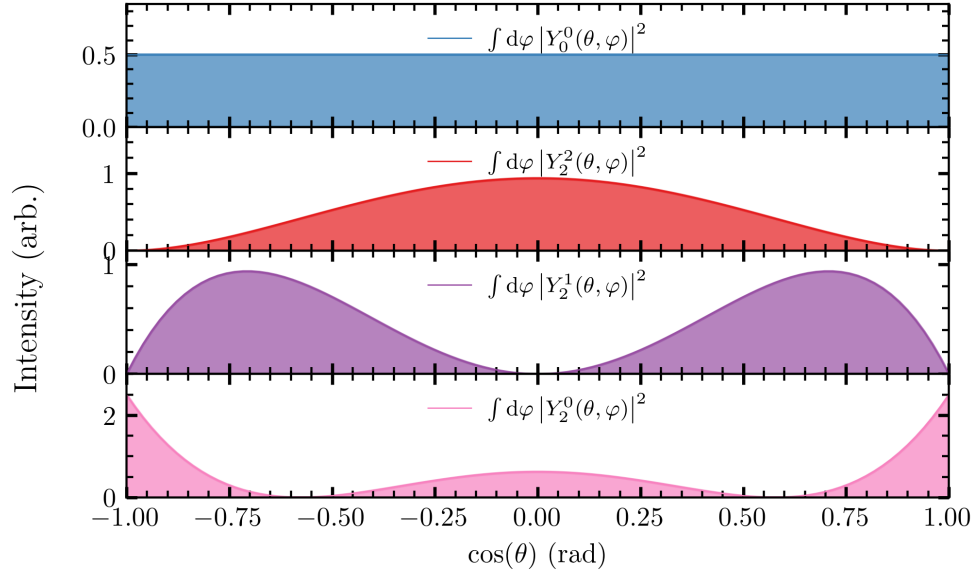


Figure 3.1: Absolute square of spherical harmonics for S- and D-waves integrated over φ .

Including Linear Polarization

3.3 The Z_ℓ^m Amplitude

3.4 The K -Matrix Parameterization

3.5 Waveset Selection

Chapter 4

Results and Systematic Studies

4.1 Mass-Independent Fits

4.2 Mass-Dependent Fits

4.3 Systematics

Chapter 5

Conclusion

Appendix A

Derivation of the Chew-Mandelstam Function

We begin with the dispersion integral¹:

$$C(s) = C(s_{\text{thr}}) - \frac{s - s_{\text{thr}}}{\pi} \int_{s_{\text{thr}}}^{\infty} ds' \frac{\rho(s')}{(s' - s)(s' - s_{\text{thr}})} \quad (\text{A.1})$$

where $s_{\text{thr}} = (m_1 + m_2)^2$ and

$$\rho(s) = \sqrt{\left(1 - \frac{(m_1 + m_2)^2}{s}\right) \left(1 - \frac{(m_1 - m_2)^2}{s}\right)} \quad (\text{A.2})$$

We first focus on just the integral part:

$$I(s) = \int_{s_{\text{thr}}}^{\infty} ds' \frac{\rho(s')}{(s' - s)(s' - s_{\text{thr}})} \quad (\text{A.3})$$

$$\lim_{\epsilon \rightarrow 0} \int_a^b dx \frac{f(x)}{(x - x_0) + i\epsilon} = \oint_a^b dx \frac{f(x)}{(x - x_0)} + i\pi f(x_0) \quad (\text{A.4})$$

$$I(s) = \oint_{s_{\text{thr}}}^{\infty} \quad (\text{A.5})$$

¹see [arXiv paper](#)